EXPERIMENTAL STUDY OF HEAT TRANSFER THROUGH COOLING WATER CIRCUIT IN A REACTOR VAULT BY USING AL_2O_3 NANOFLUID

by

Maria ANISH [a*] ***and Balakrishnan KANIMOZHI*** [b]

[a] Department of Mechanical Engineering, Sathyabama University, Jeppiaar Nagar, Chennai, India
[b] School of Mechanical Engineering, Sathyabama University, Jeppiaar Nagar, Chennai, India

Original scientific paper
https://doi.org/10.2298/TSCI170527207A

The heat produced in the nuclear reactor due to fission reaction must be kept in control or else it will damage the components in the reactor core. Nuclear plants are using water for the operation dissipation of heat. Instead, some chemical substances which have higher heat transfer coefficient and high thermal conductivity. This experiment aims to find out how efficiently a nanofluid can dissipate heat from the reactor vault. The most commonly used nanofluid is Al_2O_3 nanoparticle with water or ethylene as base fluid. The Al_2O_3 has good thermal property and it is easily available. In addition, it can be stabilized in various PH levels. The nanofluid is fed into the reactor's coolant circuit. The various temperature distribution leads to different characteristic curve that occurs on various valve condition leading to a detailed study on how temperature distribution carries throughout the cooling circuit. As a combination of Al_2O_3 as a nanoparticle and therminol 55 as base fluid are used for the heat transfer process. The Al_2O_3 nanoparticle is mixed in therminol 55 at 0.05 vol.% concentration. Numerical analysis on the reactor vault model was carried out by using ABAQUS and the experimental results were compared with numerical results.

Key words: *Al_2O_3 nanoparticles, convective radiation, heat dissipation, therminol, nuclear reactor, inert gases, nanofluids, sonification, reactive plates*

Introduction

Reactor vault (RV) is an important structure supporting the main and safety vessels of the reactor. It is a thick cylindrical structure built around the safety vessel. The RV is lined with a carbon steel liner on the side facing the safety vessel [1]. The heat from the RV is removed by demineralized cooling water flowing through square pipes welded on liner plate and embedded in RV. The cooling water removes the heat from the concrete and liner plate. The RV of fast breeder test reactor is divided into two walls, viz. the inner wall is of 750 mm thickness while the outer wall is of 1000 mm thickness. Between these two walls, 50 mm thick expanded polystyrene (EPS) insulation is sandwiched. However, the inner layer supports only the safety vessel. The sandwich could also accommodate free differential movement of the two walls and keep the outer wall cool. The temperature difference between the inner and the outer faces of these layers are essential to estimate thermal stresses. These temperature differences

* Corresponding author, e-mail: anish2010me@gmail.com

depend upon the sandwich material between the two layers of the concreate section. The EPS is taken as an insulator to reduce the temperature difference within the walls. It also maintains the outer wall at cooler temperature. A parametric study on the thickness of the EPS leads to the conclusion that, a 50 mm thick EPS insulation is adequate to provide acceptable temperature distribution [2]. The objective of this present work is to do thermal analysis for entire length of the RV [3].

Reactor vault cooling system

For the purpose of cooling, the RV is cooled by five square cooling pipes. The cooling tubes of each region are divided into two loops with alternate pipes connected to one loop [4, 5]. This ensures that, in case of leakage in any one of the loops, the other loop supports to maintain the heat transfer rate. This arrangement leads to any one of the following combinations of consecutive cooling pipes. Cooling pipe, followed by another cooling pipe – this is referred to as the WWWWW case. This occurs when pipes of both the loops in adjacent segments are working cooling pipe, followed by a non-cooling pipe and then a cooling pipe – this is referred to as the WNWNW case. This occurs when the pipes of one particular loop are not working when all the pipes are not working it is referred as NNNNN case. This occurs when all the pipes attached to alternate loops in two adjacent loops are not working based on earlier parametric studies, the pitch of the cooling pipes is fixed as 200 mm and the size of the square pipe is 25 mm × 25 mm × 3.2 mm [6, 7].

Liner plate and cooling circuit

The liner plate is made up of mild steel plate of dimensions of 1100 ×1100 ×6 mm. Five numbers of square section cooling pipes of dimension 25 × 25 × 3 mm are welded to the liner plate at a pitch of 200 mm. The square pipes are connected to three headers such as top header and two bottom headers. The outlet of the top header is connected to the heat exchanger. The inlet and the outlet of heat exchanger is connected to the water tank. A 0.5 hours power pump is provided in the tank to circulate water through the circuit [8, 9]. Two square pipes are connected to the bottom left side header and three square pipes are connected bottom right side header. The bottom headers receive water from the tank with the help of a pump. Each inlet pipe is provided with pressure gauge and control valve to regulate the flow of water through the circuit [10]. A by-pass valve is also inserted at the pump outlet to control the flow of water through the circuit [11, 12]. The flow meters are provided in the square pipes to measure the water flow rate, fig. 1.

When the water passes through the square pipes welded to the liner plate it gets heated and the hot water is sent to top header and from this header, the water flows through the heat exchanger where it is cooled and supplied to the tank. Water is re-circulated through the circuit with the help of a pump, fig. 2.

Experimental preparation of Al_2O_3-therminol 55 nanoheat transfer fluid (nHTF)

Spherical Al_2O_3 nanoparticle with 99.5% purity with reactive index of 1.768 and surface area of 32-40 m^2/g are used to prepare nHTF [13]. The surface morphology and microstructure of the nanoparticle are observed using electron microsope. The SEM images of Al_2O_3 at 200.00x and 30.00x are shown in the fig. 3 [14]. The nanoparticle used in this process has an average size of 30-40 mm. Therminol 55 has good miscibility and viscosity so it is used as a base fluid. The amount of nanoparticle to be added to achieve a concentration of 0.05 is obtained using the eq. (1).

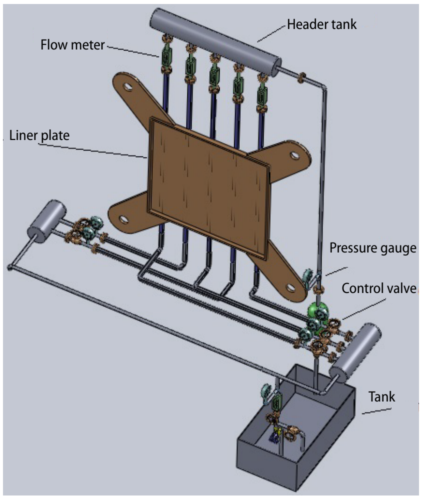

Figure 1. Cooling water circuit

Figure 2. Photographic view of reator vault

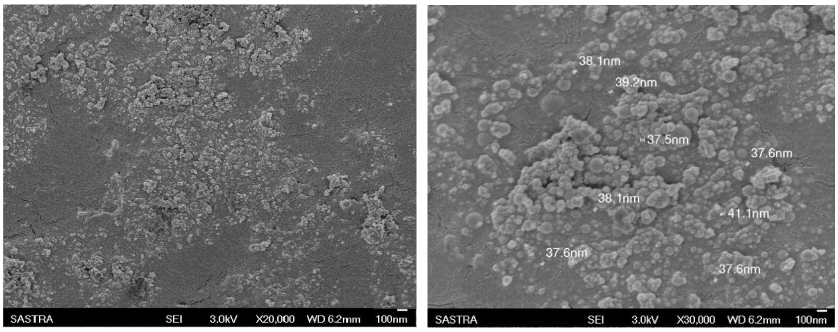

Figure 3. The SEM images at 20000x X20,000and 30000x X30,000 magnification of Al_2O_3 nanoparticle

$$\phi = \frac{\dfrac{W(Al_2O_3)}{3950}}{\dfrac{W(Al_2O_3)}{3950} + \dfrac{\text{Quantity of therminol [ml]}}{\text{Density of therminol [kgm}^{-3}\text{]}}}$$

$$\frac{0.05}{100}\frac{W(Al_2O_3)}{3950} + \frac{1000}{868} = \frac{W(Al_2O_3)}{3950} \tag{1}$$

$$W(Al_2O_3) = 2.25 \text{ g} \tag{2}$$

The 2.25 g of Al_2O_3 nanoparticle is measured using electronic weighing machine which is dispersed in one liter of therminol 55 base fluid. Then the mixture is kept in magnetic stirrer which is left for around 15-25 minutes. So the nanoparticle completely disperse into the base fluid.

Figure 4 shows the magnetic stirring of nanoparticle in therminol base fluid. The 2.25 g of Al_2O_3 nanoparticle is added to one liter of therminol which is kept over the magnetic stirrer [15, 16]. A small roller bearing is dropped inside the beaker and aligned to center position. When the intensity of the magnetic stirrer is increased the roller begins to produce a tornado. The tornado causes an effective dispersing of nanoparticle and base fluid. This process is allowed to take place for 15-20 minutes, depending on volumen concentration of the nanofluid. Figure 5 shows the ultrasonic bath apparatus for stabilization of the nanofluid. Nanofluid ultrasonic bath is carried out in order to maintain the stability in the nanofluid. After the magnetic stirrer process, one liter of nanofluid is separated into 2 half liters and placed in the ultrasonic bath apparatus which is filled with distilled water. The temperature of the process is set to 30 ºC and the total time of the process is set through the timer as 25 minutes.

Figure 4. The magnetic stirrer

Figure 5. Ultrasonic bath for stabilization of nanofluid

The ultrasonic stabilization process is necessary in order to maintain the stability of the nanofluid. Or else nanofluid can lose their potential to transfer heat. The stability method used in this process is ultrasonic bath. Then the mixture is kept in the ultrasonic bath for 30-40 minutes in order to improve the stability of the nanofluid and this process is known as sonification. This process is used to prepare nanofluid of Al_2O_3-therminol 55 combination with a volumetric concentration of 0.05% [17, 18].

Thermocouple location in cooling water circuit and RV

A thermocouple is a temperature-measuring device consisting of two dissimilar conductors that contact each other at one or more spots, where a temperature differential is experienced by the different conductors (or semiconductors). It produces a voltage when the temperature of one of the spots differs from the reference temperature at other parts of the circuit. Thermocouples are widely used temperature sensor for measurement and control, and it can also convert a temperature gradient into electricity. A total of 64 numbers of K-type thermocouples are used in this set-up in order to measure the temperature at different locations. Thermocouples are fastened to five locations on each plate with the help of a nut. The nuts are welded to each plate with the help of arc welding, fig. 6.

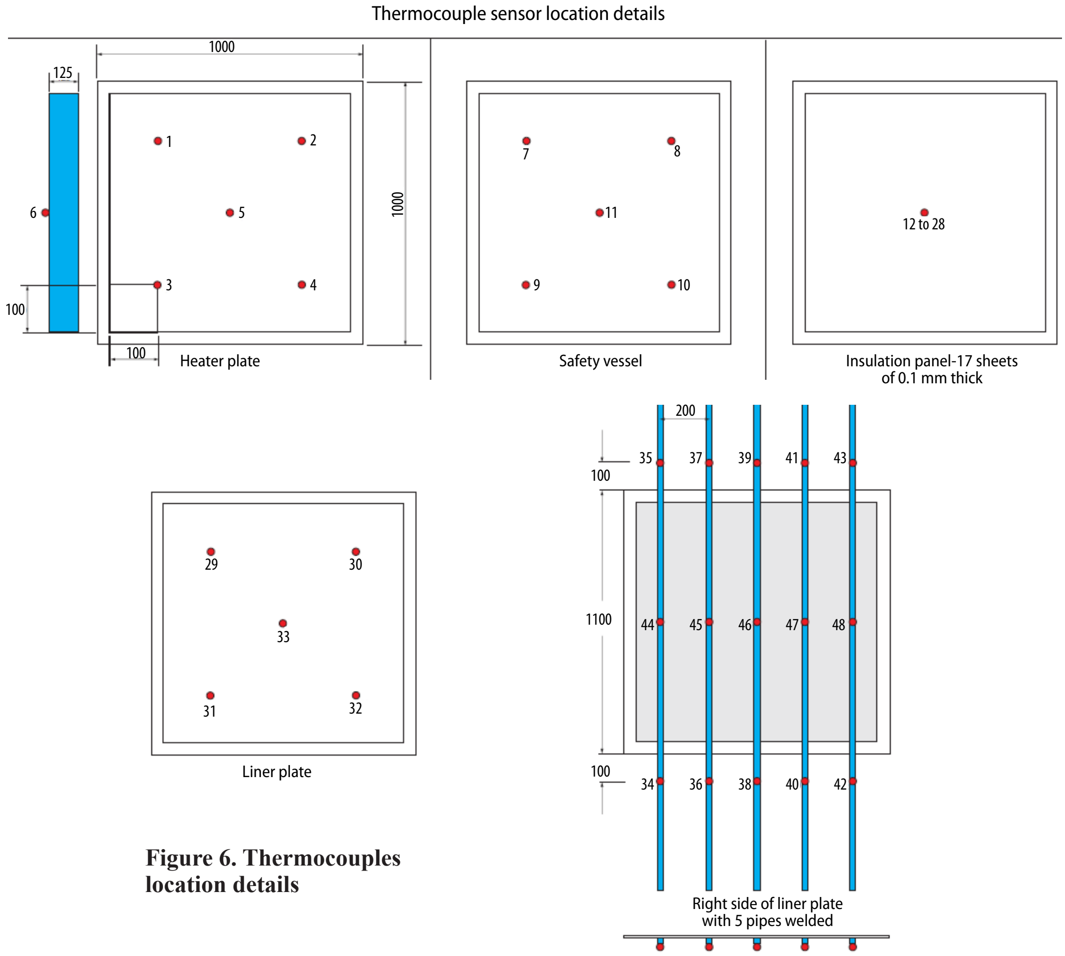

Figure 6. Thermocouples location details

Experimental methodology

An experimental program has been undertaken in the model to study the temperature distribution at various locations in the main vessel, safety vessel, thermal insulation, liner, cooling pipes, and concrete. The experiments are conducted to maintain the main vessel at different temperature level of 100 °C, 200 °C, 300 °C, 400 °C, 500 °C, and 577 °C along with five cooling pipes. The experiments are also conducted by maintaining the main vessel at different temperature with alternate cooling which pipes are not working. The cooling nanofluid flow rate through the pipes welded to liner plate is maintained at 6 lpm.

Experimental results

The temperature at 64 locations in the model has been noted down at steady-state condition. The temperature distribution graphs are plotted with respect to sensor locations.

Discussion of experimental results

In this trial, the temperature of main vessel (heater plate) is set at 577 ºC and the temperature at various locations of the model has been noted at steady-state condition. It is found

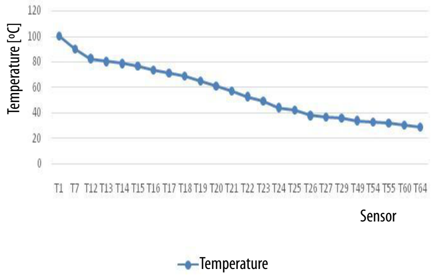

Figure 7. Temperature distribution when main vessel is set at 100 °C

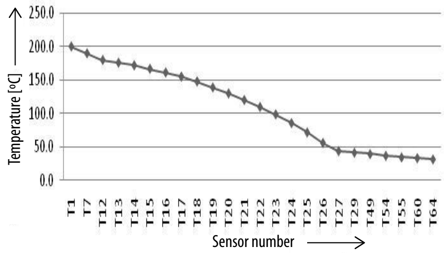

Figure 8. Temperature distribution when main vessel is set at 200 °C

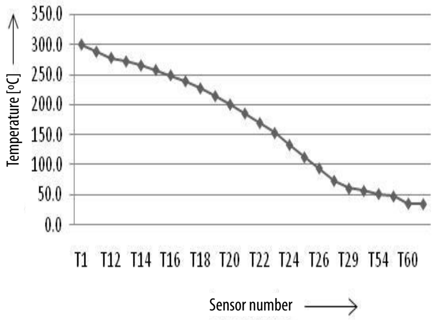

Figure 9. Temperature distribution when main vessel is set at 300 °C

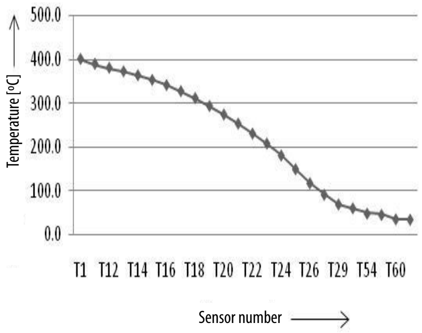

Figure 10. Temperature distribution when main vessel is set at 400 °C

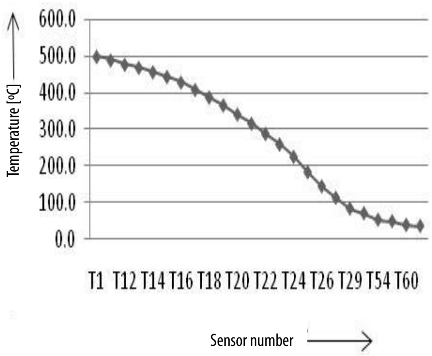

Figure 11. Temperature distribution when main vessel is set at 500 °C

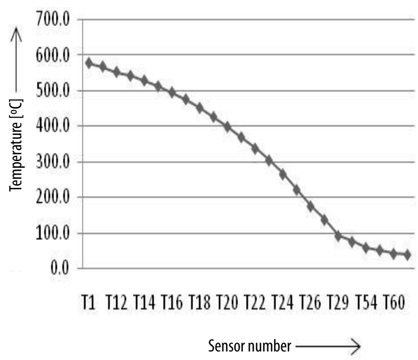

Figure 12. Temperature distribution when main vessel is set at 577 ºC

that the temperature of safety vessel – MS plate temperature (sensor T7 as 567 °C), insulation panel temperature ranging from T12 as 552 °C and T27 as 134.9 °C, liner temperature T29 as 89 °C, concrete vault temperature T49 as 73 °C , T54 as 56 °C, T55 as 49 °C, T60 as 39 °C, and T64 as 36 °C. The temperature distribution graph with respect to sensor locations is shown, figs. 7-12.

Numerical analysis as validation of experimental results

Methodology for numerical analysis

Numerical analysis of the model has been done by using ANSYS CFD. The steps in the analysis are.

The property module

The properties of the materials for the different parts of the model are assigned using PROPERTY module [19]. The following properties are assigned, tab. 1.

Table 1. Properties of materials used in RV

Materials	Conductivity [W/mm°C]	Specific heat [J/kg°C]	Density [kg/mm^3]
Stainless steel 304L plate	0.00006	490	8.03E-6
N_2	0.000026	1040	1.153E-9
Concrete	0.0008	420	2.4E-6
EPS	3.3E-5	1.3	1E-6
MS plate	0.00006	510	8.03E-6

Mesh module

The mesh module allows generating meshes on parts and assemblies created within ANSYS/CAE. Various levels of automation and controls are available so that a mesh that meets the needs of the analysis can be created. The mesh module provides the following features: Tools for prescribing mesh density at local and global levels. Model coloring that indicates the meshing technique assigned to each region in the model [20, 21]. A variety of mesh controls, such as: element shape, meshing technique, meshing algorithm, adaptive re-meshing rule, fig. 13.

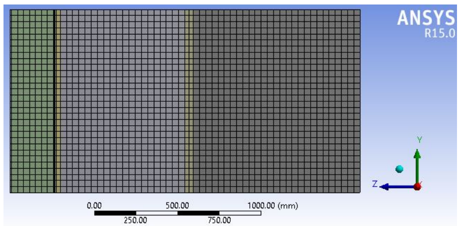

Figure 13. Meshed image of the set-up using hypermesh

In the numerical analysis, the temperature of main vessel (heater plate) is set at 577 °C and the temperature at various locations of the model are analyzed. It was found that the temperature of safety vessel – MS plate temperature (sensor T7 as 554 °C), insulation panel temperature ranging from T12 as 529 °C and T27 as 103 °C, liner temperature T29 as 80 °C, concrete vault temperature T54 as 48 °C, T55 as 43 °C, T60 as 38 °C, and T64 as 36 °C. The temperature distribution graph with respect to sensor locations is shown figs. 14-19.

Comparison of experimental and numerical analysis

Figures 20-25 shows the comparison of temperature distribution obtained by experimental and numerical analysis. The temperature values obtained by numerical analysis were

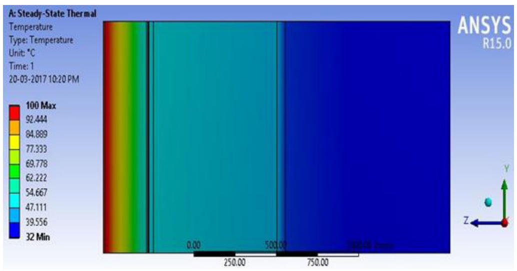

Figure 14. Temperature distribution when main vessel is set at 100 °C

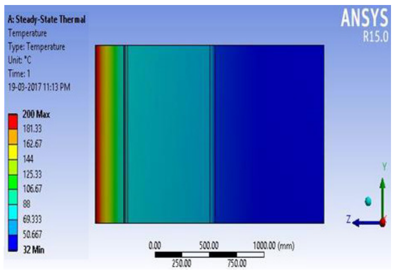

Figure 15. Temperature distribution when main vessel is set at 200 °C

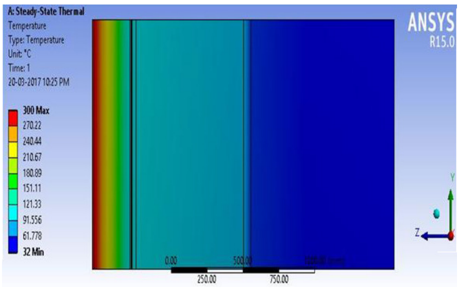

Figure 16. Temperature distribution when main vessel is set at 300 °C

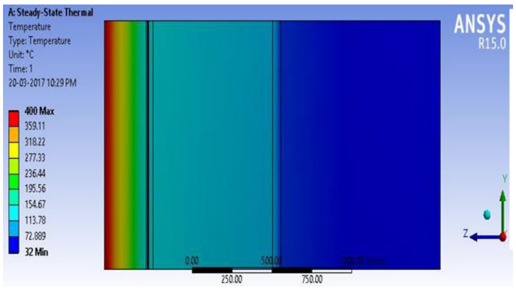

Figure 17. Temperature distribution when main vessel is set at 400 °C

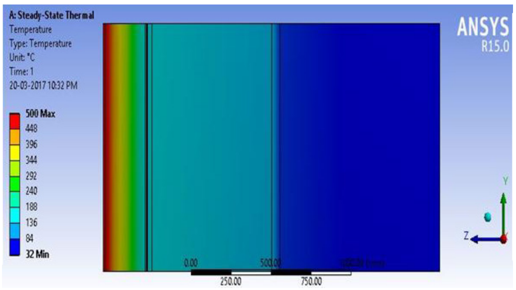

Figure 18. Temperature distribution when main vessel is set at 500 °C

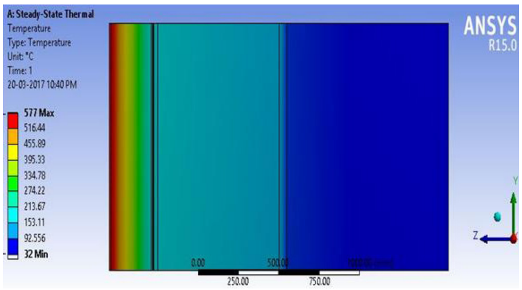

Figure 19. Temperature distribution when main vessel is set at 577 °C

found to be slightly less or equal to experimental values. So the experimental results can be validated by numerical analysis. An experimental program has been undertaken in the model to study the temperature distribution at various locations in the main vessel, safety vessel, thermal insulation, liner, cooling pipes, and concrete. The experiments are conducted by maintaining the main vessel at different temperature level of 100 °C, 200 °C, 300 °C, 400 °C, 500 °C , and 577 °C with all the five cooling pipes which are working. The experiments are also conducted by maintaining the main vessel at different temperature with alternate cooling pipes which are not working. The cooling nanofluid flow rate through the pipes welded to liner plate is maintained at 6 lpm. The temperature at 64 locations in the model are noted down at steady-state condition. The temperature distribution graphs are plotted with respect to sensor locations.

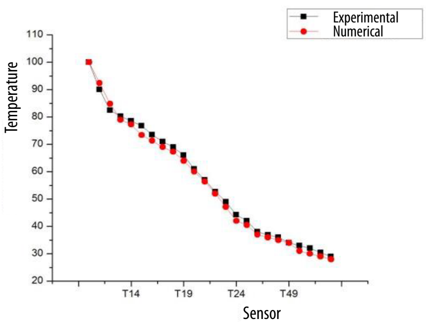

Figure 20. Comparison of experimental and numerical values when main vessel is set at 100 °C

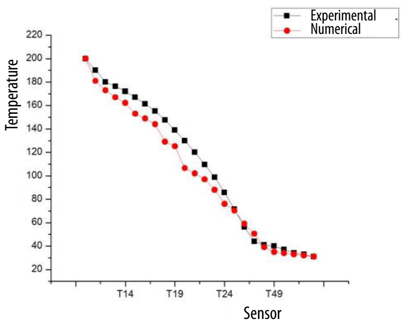

Figure 21. Comparison of experimental and numerical values when main vessel is set at 200 °C

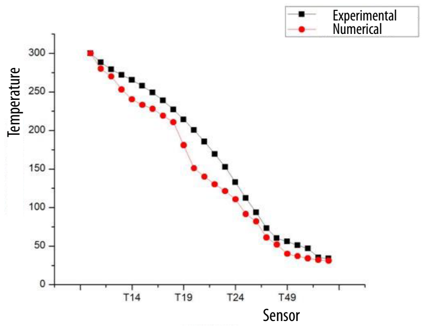

Figure 22. Comparison of experimental and numerical values when main vessel is set at 300 °C

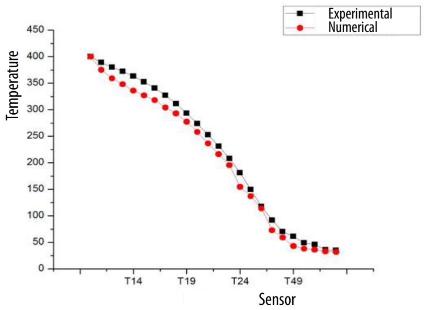

Figure 23. Comparison of experimental and numerical values when main vessel is set at 400 °C

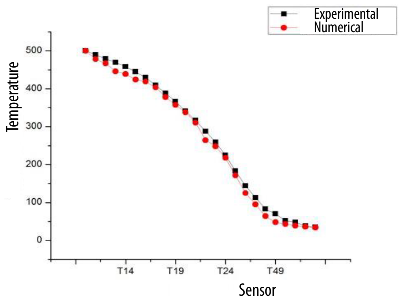

Figure 24. Comparison of experimental and numerical values when main vessel is set at 500 °C

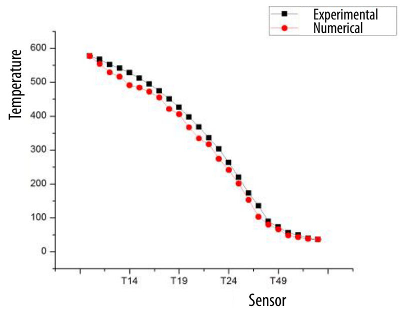

Figure 25. Comparison of experimental and numerical values when main vessel is set at 577 °C

In this trial, the temperature of main vessel (heater plate) is set at 200 °C and the temperature at various locations of the model has been noted at steady-state condition. The fig. 20-25 shows the temperature distribution in the cooling water circuit. The temperature difference between the inlet and outlet of cooling pipes has been found to be 2 °C, figs. 26-31.

Comparison between experimental results when all the cooling pipes are opened and when the alternate pipes are closed

The temperatures measured at different locations were found to be almost equal for WWWWW condition and WNWNW condition except near the liner plate, where the temperature was slightly higher for WNWNW condition, figs. 32-37.

Temperature distribution calculations

The water velocity through the pipes is 0.105 m/s and the Reynolds number of the flow is 3000. The Nusselt number and hence the heat transfer coefficient for water side in cooling circuit is calculated:

$$\mathrm{Nu} = \frac{\dfrac{f}{8}(\mathrm{Re}-1000)\,\mathrm{Pr}}{1+12.7\sqrt{\dfrac{f}{8}}\,(\mathrm{Pr}^{2/3}-1)} \quad \text{and} \quad \frac{f}{4} = 0.0054 + \frac{2.3\cdot 10^{-8}}{\mathrm{Re}^{-3/2}} \tag{3}$$

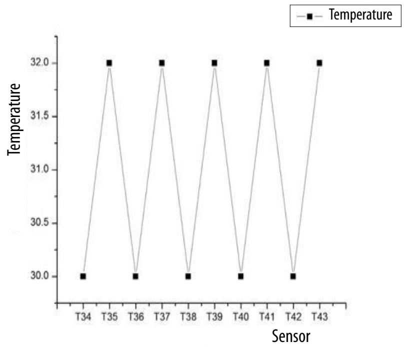

Figure 26. Temperature distribution of cooling fluid circuit at 100 °C

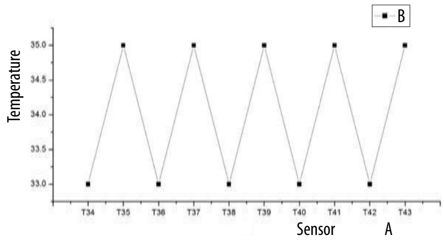

Figure 27. Temperature distribution of cooling fluid circuit at 200 °C

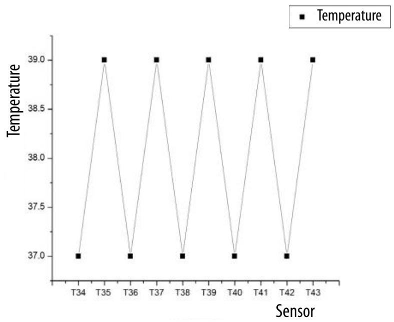

Figure 28. Temperature distribution of cooling fluid circuit at 300 °C

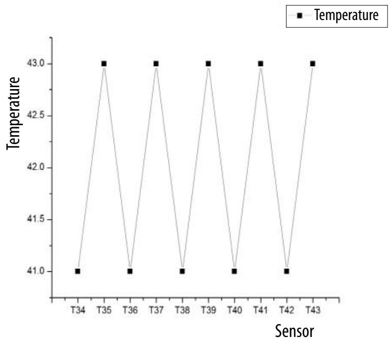

Figure 29. Temperature distribution of cooling fluid circuit at 400 °C

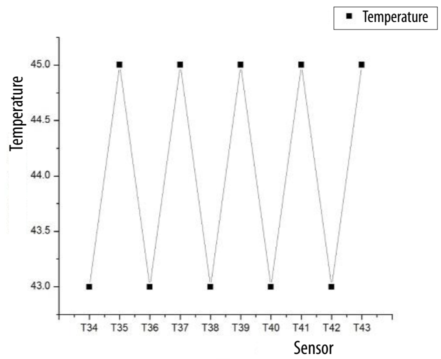

Figure 30. Temperature distribution of cooling fluid circuit at 500 °C

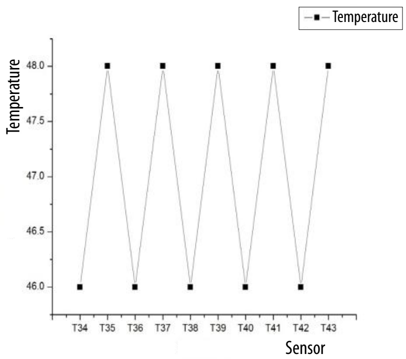

Figure 31. Temperature distribution of cooling fluid circuit at 577 °C

where f is the Darcy's friction factor, Re – the Reynolds number, and Pr – the Prandtl number of water

Discusion of experimental *vs.* numerical results

From the experimental study and numerical, the following conclusions were drawn.

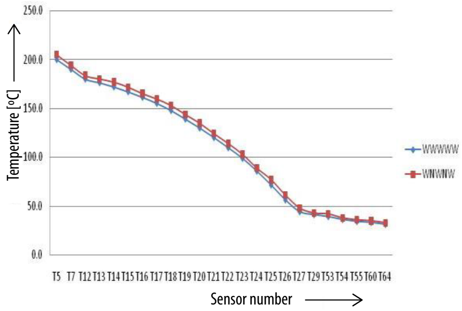

Figure 32.

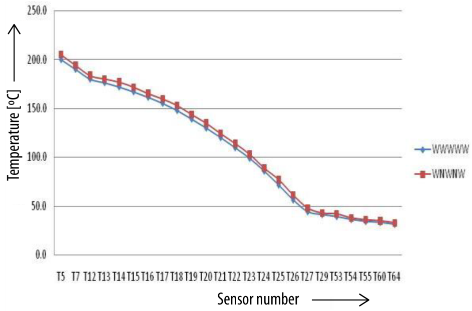

Figure 33.

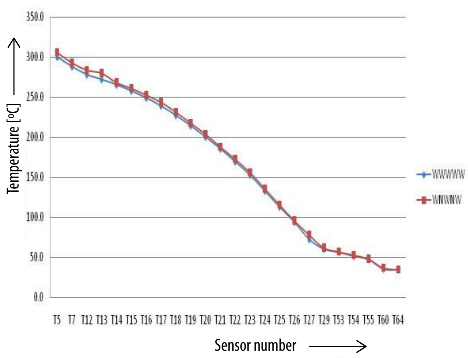

Figure 34.

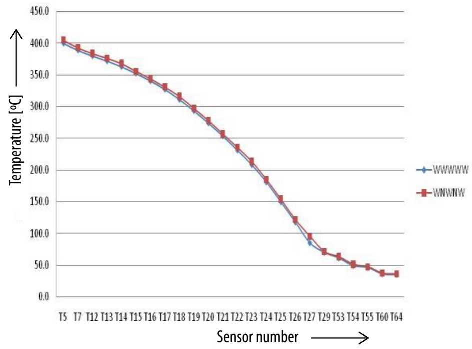

Figure 35.

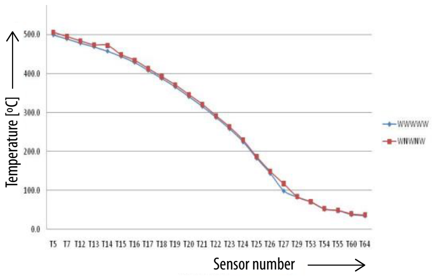

Figure 36.

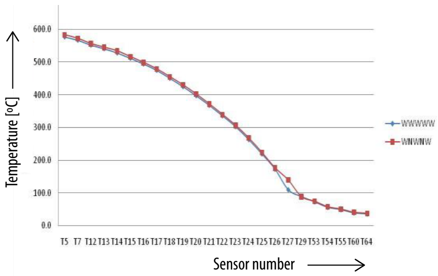

Figure 37.

Figures 32-37. Shows the comparison between experimental results when all the cooling pipes opened and when the alternate pipes are closed when main vessel is set at 100 °C to 577 °C

When the temperature of main vessel (heater plate) was set at 100°C, the temperatures at inner and outer faces of the inner concrete vault were 40 °C (T49) and 34 °C (T55), respectively, and the difference was 5 °C which is less than acceptable temperature difference. When the temperature of main vessel (heater plate) was set at 100 °C, the temperature at T55 was 36 °C and at T60 was 33 °C. When the temperature of main vessel (heater plate) was set at 200 °C, the temperatures at inner and outer faces of the inner concrete vault were 41 °C (T49) and 36 °C (T55), respectively, and the difference was 5 °C which is less than acceptable temperature difference. When the temperature of main vessel (heater plate) was set at 200 °C, the temperature at T55 was 37 °C and at T60 was 34 °C. When the temperature of main vessel (heater plate) was set at 300 °C, the temperatures at inner and outer faces of the inner concrete vault were 56 °C (T49) and 47 °C (T55), respectively, and the difference was 9 °C which is less than acceptable temperature difference. When the temperature of main vessel (heater plate) was set at 300 °C, the temperature at T55 was 47 °C and at T60 was 35 °C. When the temperature of main vessel (heater plate) was set at 400 °C, the temperatures at inner and outer faces of the inner concrete vault were 61 °C (T49) and 46 °C (T55), respectively, and the difference was 15 °C which is less than acceptable temperature difference. When the temperature of main vessel (heater plate) was set at 400 °C, the temperature at T55 was 46 °C and at T60 was 36 °C. When the temperature of Main vessel (heater plate) was set at 500 °C, the temperatures at inner and outer faces of the inner concrete vault were 70 °C (T49) and 48 °C (T55), respectively, and the difference was 22 °C which is less than acceptable temperature difference.

When the temperature of main vessel (heater plate) was set at 500 °C, the temperature at T55 was 48 °C and at T60 was 38 °C. When the temperature of main vessel (heater plate) was set at 577 °C, the temperatures at inner and outer faces of the inner concrete vault were 72 °C (T49) and 49 °C (T55), respectively, and the difference was 23 °C which is less than acceptable temperature difference. When the temperature of main vessel (heater plate) was set at 577 °C, the temperature at T55 was 49 °C and at T60 was 39 °C. When heat is transferred from inner face of inner concrete vault to end face of outer concrete vault, there is a large temperature difference taking place between the inner concrete vault and outer concrete vault (between T55 and at T60) due to the presence of EPS sheet for which the conductivity is less. Hence, the temperature at the outer face of the outer vault is maintained slightly above the room temperature in all cases.

Conclusion

Experimental study was carried out on the set-up by maintaining the main vessel at different temperatures with all the cooling pipes working and with alternate cooling pipes not working. The temperatures were measured at 64 locations in the set-up at steady-state condition. The water circulation through the square pipes welded to liner plate was maintained at 6 lpm. Numerical analysis on the model was carried out using ABAQUS and the experimental results were compared with numerical results. The temperatures obtained by numerical analysis were found to be slightly less or equal to experimental temperature values when the main vessel was set at different temperatures. From this experiment we found that the cooling circuit with nanofluid in RV will absorb more heat compared to water. Thus the experimental results were validated by numerical analysis.

Nomenclature

Nu – Nusselt number, [–]
Re – Reynolds number, [–]

Acronyms

EPS – expanded polystyrene
nHTF – nanoheat transfer fluid
SS-GRADE 304 – stainless steel- GRADE 304

References

[1] El-Hosiny, F. I., El-Faramawy, N. A., Shielding of Gamma Radiation by Hydrated Portland Cement-Lead Pastes, *Radiation Measurements, 32* (2000), 2, pp. 93-99
[2] El-Khayatt, A. M., Radiation Shielding of Concretes Containing Different Lime/Silica Ratios, *Annals of Nuclear Energy, 37* (2010), 7, pp. 991-995

[3] Kharita, M. H., *et al*., Development of Special Radiation Shielding Concretes Using Natural Local Materials and Evaluation of Their Shielding Characteristics, *Progress in Nuclear Energy, 50* (2008), 7, pp. 33-36
[4] Armelin, H. S., Cherry, N., Evaluation of the Use and Performance of Thermal Radiation Barriers in Construction, *E-Magazine Mat., 1* (2004), 1, pp. 79-82
[5] Bajorek, S. M., Lloyd, J. R., Experimental Investigation of Natural Convection in Partitioned Enclosures, *Journal of Heat Transfer, 104* (1982), 3, pp. 527-531
[6] Ciofalo, M., Karayiannis, T. G., Natural Convection Heat Transfer in a Partially – or Completely – Partitioned Vertical Rectangular Enclosure, *International Journal of Heat and Mass Transfer, 34* (1991), 1, pp. 167-179
[7] Dare, C. A. N., *et al*., Evaluating the Effectiveness of Thermal Insulation by Reflection, Used as under-Coverage, *Energ. Agric., Botucatu, 20* (2005), 2, pp. 14-29
[8] Lorente, S., Heat Losses through Building Walls with Closed, Open and Deformable Cavities, *International Journal of Energy Research, 26* (2002), 7, pp. 611-632
[9] Manz, H., Numerical Simulation of Heat Transfer by Natural Convection in Cavities of Facade Elements, *Energy and Buildings, 35* (2003), 3, pp. 305-311
[10] Akkurt, I., H., *et al*., Gamma ray Shielding Properties of Concrete Including Barite at Different Energies, *Progress in Nuclear Energy, 52* (2010), 7, pp. 620-623
[11] Akkurt, I., C. *et al.*, The Shielding of γ-Rays by Concretes Produced with Barite, *Progress in Nuclear Energy, 46* (2005), 1, pp. 1-11
[12] Gandhidasan, P., Ramamurthy, K. N., Thermal Bahaviour of Hollow-Cored Concrete Slabs, *Applied Energy, 19* (1985), 1, pp. 41-48
[13] Hafiz Muhammad, A., *et al.*, Heat Transfer Enhancement of Car Radiator Using Aqua Based Magnesium Oxide Nanofluids, *Thermal Science, 19*, (2015), 6, pp. 2039-2048
[14] Shanthi, R, *et al.*, Heat Transfer Enhancement Using Nanofluid, *Thermal Science, 16* (2012), 2, pp. 423-444
[15] Bajorek, S. M., Lloyd, J. R., Experimental Investigation of Natural Convection in Partitioned Enclosures, *Journal of Heat Transfer, 104* (2008), 3, pp. 527-531
[16] Ghouti, S., *et al.*, Dynamic Thermal Behavior of Building Using Phase Change Materials for Latent Heat Storage, *Thermal Science, 19* (2015), Suppl. 2, pp. S603-S613
[17] Ciofalo, M., Karayiannis, T. G., Natural Convection Heat Transfer in a Partially – or Completely – Partitioned Vertical Rectangular Enclosure, *International Journal of Heat and Mass Transfer, 34* (1991), 1, pp. 167-179
[18] De Graff, J. G. A., van der Held, E. F. M., The Relation between the Heat Transfer and the Convection Phenomena in Enclosed Plane Air Layers, *Applied Scientific Research, 3* (1952), 6, pp 393-409
[19] Del Coz Diaz, J. J., *et al*., Analysis and Optimization of the Heat-Insulating Light Concrete Hollow Brick Walls Design by the Finite Element Method, *Applied Thermal Engineering , 27* (2007), 4, pp. 1445-1456
[20] France, D. M., *et al.*, Thermophysical Property-Related Comparison Criteria for Nanofluid Heat Transfer Enhancement in Turbulent Flow, *Applied Physics, 96* (2010), 213109
[21] Zeinali Heris, S., *et al.*, Experimental Investigation of Convective Heat Transfer of Al_2O_3/Water Nanofluid in Circular Tube, *International Journal of Heat Flow, 28* (2007), 2, pp. 203-210

Paper submitted: May 27, 2017
Paper revised: September 7, 2017
Paper accepted: September 25, 2017